Metal–Organic Capsules

DOI: 10.1002/anie.200804255

Metal–Organic Spheres as Functional Systems for Guest Encapsulation**

*Inhar Imaz, Jordi Hernando, Daniel Ruiz-Molina, and Daniel Maspoch**

The encapsulation of functional species within micro- and nanometer-sized matrices has great potential in the areas of drug delivery and cosmetics,[1,2] medical diagnostics,[3,4] and materials science.[5,6] Many different materials have been used as matrices that satisfy all the critical properties needed for each intended application; a variety of capsules such as liposomes,[7] cyclodextrins,[8] chitosan,[9] organic polymeric particles,[10] dendrimers,[11] and carbon- or silicate-based hollow spheres[12] have been used. To date, however, the use of metal–organic micro- and nanoparticles as encapsulating matrices has not been explored. Metal–organic solids created by the association of metal ions and multitopic organic ligands are a very promising type of materials because of their broad compositional and structural diversity, low cost, and facile production. Their wide range of potential properties and applications include gas sorption, catalysis, ion exchange, sensing, drug-delivery, magnetism, fluorescence, and nonlinear optics.[13] Because of this rich range of properties, we envisaged the use of conventional metal–organic chemistry in the fabrication of functional matrices that display the intrinsic properties of such molecular materials.

Prior to this work, advances were made in the miniaturization of metal–organic materials to the micro- and nanometer scale.[14,15] Among these examples, an alternative and promising methodology has been recently reported by Oh and Mirkin[16] and Wang and co-workers.[17] This strategy, which is based on infinite coordination polymerization[16] followed by precipitation with a poor solvent, allows the straightforward fabrication of cross-linked submicrometer functional metal–organic spheres.[18] This approach has so far been exploited to prepare fluorescent metal–organic spheres that show selective cation-exchange[19] and hydrogen-storage properties,[20] as well as other examples with an interesting valence tautomeric behavior.[21] This fabrication process inspired us to develop a new and versatile method that utilizes metal–organic polymeric micro- and nanospheres as novel functional encapsulating matrices. Figure 1 shows our one-step strategy: novel blue-fluorescent metal–organic spheres are formed by infinite coordination polymerization of Zn^{II} metal ions and 1,4-bis(imidazol-1-ylmethyl)benzene (bix), followed by a fast precipitation to mechanically trap the desired functional species that are present in the reaction mixture. Following this methodology, the wide-ranging encapsulation capability of such spheres is demonstrated for several types of functional species, such as magnetic nanoparticles, organic dyes, and luminescent quantum dots (QDs).

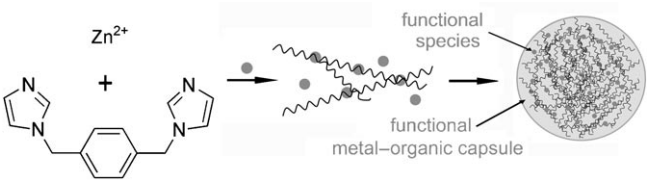

Figure 1. Schematic illustration of the simultaneous formation and encapsulation of functional species in metal–organic Zn(bix) micro- and nanospheres.

Bare metal–organic matrices in the form of micro- and nanospheres (hereafter referred to as Zn(bix) spheres) were initially investigated and prepared by addition of an aqueous solution of $Zn(NO_3)_2{\cdot}6H_2O$ to an ethanolic solution of bix (in a 1:1 molecular ratio) with vigorous stirring at room temperature. After 5 minutes, ethanol was added to the reaction mixture to stabilize the particles. Zn(bix) spheres were then purified by centrifugation and washed several times with ethanol, and finally redispersed in ethanol. The resulting white colloid showed a remarkable stability, as the first traces of aggregation appeared after more than one month. Furthermore, degradation of the particles in ethanol over this period was not observed. Scanning (SEM) and transmission (TEM) electron microscopy images of the colloid demonstrated the formation of spherical particles with uniform diameters in the range 100–1500 nm (Figure 2a), depending on the concentration of the reactants. For example, colloidal Zn(bix) spheres with average diameters of (1050 ± 83) nm, (600 ± 68) nm, (270 ± 33) nm, and (130 ± 14) nm were systematically synthesized by increasing the concentration of both $Zn(NO_3)_2{\cdot}6H_2O$ and bix components from 5×10^{-3} M to 1×10^{-2} M, 2.5×10^{-2} M, and 1×10^{-1} M, respectively. The average diameters of all these particles were further confirmed by dynamic light scattering (DLS) measurements (Figure 2d).

[*] Dr. I. Imaz, Dr. D. Ruiz-Molina, Dr. D. Maspoch
Centro de Investigación en Nanociencia y Nanotecnología (ICN-CSIC)
Campus UAB, 08193 Bellaterra (Spain)
Fax: (+34) 93-581-4411
E-mail: daniel.maspoch.icn@uab.es
Dr. J. Hernando
Departament de Química, Universitat Autònoma de Barcelona
Campus Universitari de Bellaterra, 08193 Bellaterra (Spain)

[**] This work was supported by projects MAT2006-13765-C02 and CTQ2006-01040. D.M. and J.H. thank the Ministerio de Ciencia y Tecnología for a RyC contract. I.I. thanks the Institut Català de Nanotecnologia for a research contract. We thank the Servei de Microscopia of the UAB and the Laboratori de Nanotecnologia of MATGAS.

Supporting information for this article is available on the WWW under http://dx.doi.org/10.1002/anie.200804255.

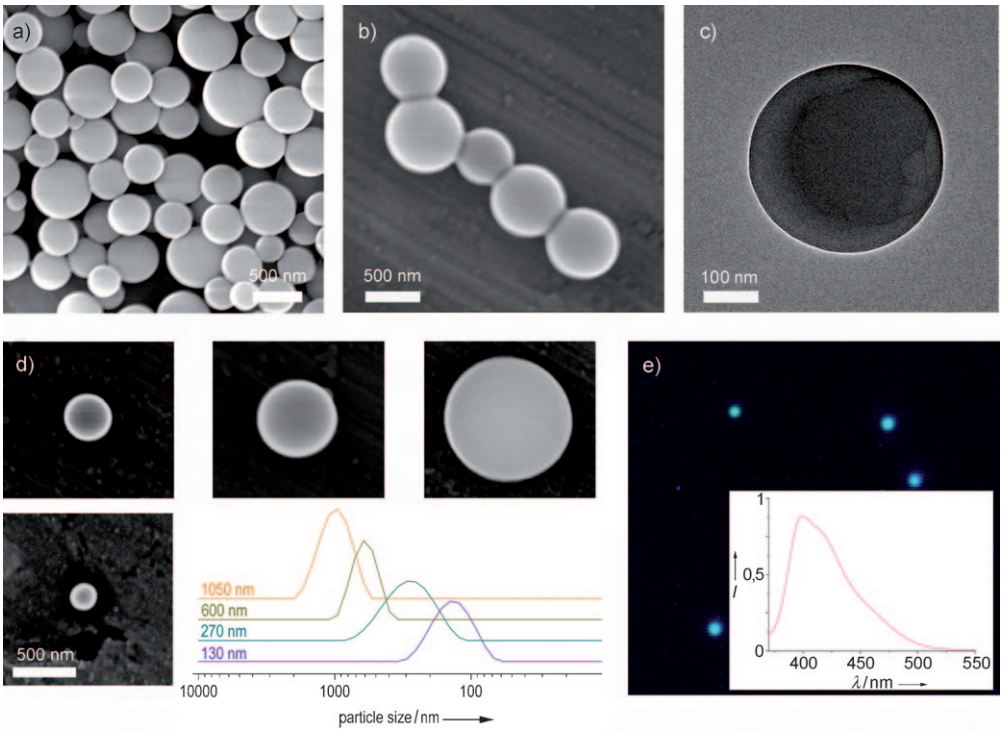

Figure 2. a, b) SEM micrographs of Zn(bix) spheres. c) High-resolution TEM image of an individual Zn(bix) sphere. d) DLS measurements of different ethanolic colloids of Zn(bix) spheres with different average diameters ((1050 ± 83) nm, (600 ± 68) nm, (270 ± 33) nm, and (130 ± 14) nm) and corresponding representative SEM images. e) Fluorescence microscope images of Zn(bix) spheres deposited onto glass (λ_{exc} = 359–371 nm, λ_{em} > 397 nm). The inset depicts the fluorescence emission spectrum collected at λ_{exc} = 355 nm.

encapsulate iron oxide nanoparticles, in which the iron oxide nanoparticles can be clearly distinguished inside the metal–organic spheres. In fact, control experiments performed by adding an ethanolic solution of iron oxide nanoparticles to a presynthesized colloidal solution of Zn(bix) spheres did not show encapsulation of the nanoparticles, but adsorption onto the external surface of the metal–organic spheres.

The chemical composition of the iron oxide nanoparticles/Zn(bix) spheres, which was determined by energy dispersive X-ray (RX-EDS) microanalysis, showed that every sphere contained zinc, iron, oxygen, nitrogen, and carbon. In addition, electron diffraction performed by TEM on commercial iron oxide nanoparticles

Similar to other examples of metal–organic spheres obtained through the infinite coordination polymerization and precipitation approach,[16,19–21] the combination of powder X-ray diffraction, IR spectroscopy, and elemental analysis performed on Zn(bix) spheres indicated that they are amorphous materials that are created from the coordination polymerization of Zn^{II} metal ions connected through bix ligands. The IR spectrum confirms coordination of bridging bix ligands to the Zn^{II} metal ions, as evidenced by the presence of two strong peaks at 1524 cm^{-1} and 1239 cm^{-1}.[22] Furthermore, the chemical composition determined by elemental analysis agrees with the formation of a polymer of formula $[Zn(bix)(NO_3)_2]$. When excited at 355 nm, the Zn(bix) spheres show strong blue luminescence with an emission peak centered at approximately 405 nm (see the inset in Figure 2e), which is also consistent with the formation of a Zn^{II}-based coordination polymer.[23] These optical properties make Zn(bix) spheres potential blue fluorescent metal–organic capsules.

In order to demonstrate the efficiency of the encapsulation process in metal–organic spheres, we first identified magnetic iron oxide particles (10 nm diameter) as good candidates for encapsulation. Zn(bix) spheres (with an average diameter of 600 nm) with entrapped iron oxide nanoparticles were fabricated by addition of an aqueous solution of $Zn(NO_3)_2 \cdot 6H_2O$ to an ethanolic solution of bix and nanoparticles under sonication at room temperature. Figure 3a, b shows TEM images of Zn(bix) spheres that

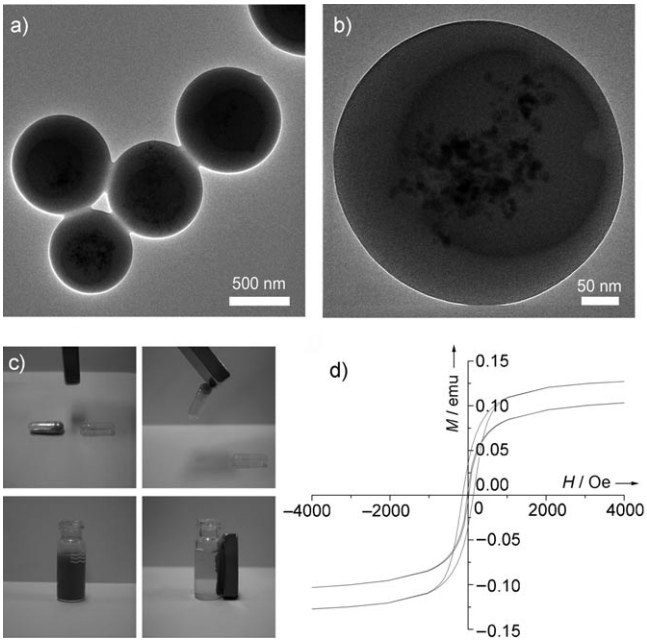

Figure 3. a,b) High-resolution TEM images of iron oxide nanoparticles/Zn(bix) spheres (nanoparticle diameter = 600 nm). c) Photographs showing the attraction of iron oxide nanoparticles/Zn(bix) nanospheres (both as a solid or colloidal solution) to a magnet. d) Magnetic hysteresis loop measured at room temperature (M_{sat} = 0.10 emu) and at 10 K (M_{sat} = 0.13 emu).

and on iron oxide nanoparticles/Zn(bix) spheres showed comparable diffraction patterns. Similarly, magnetic measurements performed on the encapsulated spheres confirmed the magnetic character of such systems, which exhibit a characteristic hysteresis loop with a coercive field of 137 Oe and 20 Oe at 10 K and at room temperature, respectively (Figure 3c,d).[24] It can therefore be concluded that the particles encapsulated within the metal–organic particles are the original iron oxide nanoparticles and that the encapsulation process does not therefore modify the nature of the embedded material. Similarly, the chemical composition, coordination polymerization, stability, and fluorescence properties of Zn(bix) spheres are not modified during the encapsulation process, as confirmed by IR and fluorescence spectroscopy and SEM studies. Interestingly, the encapsulation of functional species, such as magnetic nanoparticles, into fluorescent metal–organic capsules leads to the possibility to fabricate novel multifunctional materials at the micro- and nanometer scale by combining the functionalities of these matrices and of the encapsulated substances (Figure 3c).

To prove the generality of the in situ encapsulation and further expand the diversity of the materials encapsulated metal–organic spheres, we also investigated the encapsulation of luminescent quantum dots (QDs) and two organic dyes, fluorescein and rhodamine B. Fluorescence optical microscope images and the corresponding fluorescence spectra of QDs, fluorescein, and rhodamine B that are encapsulated by Zn(bix) spheres are shown in Figure 4a–c. All these materials were obtained by following a similar method to that used for the encapsulation of the iron oxide nanoparticles. Interestingly, encapsulation combines the inherent fluorescence properties of both Zn(bix) spheres and the trapped substances. Fluorescein/Zn(bix) particles are fluorescent in the blue and green regions of the spectrum when excited in the UV region, whereas the spheres that contain entrapped rhodamine B or QDs emit both blue and red fluorescence under the same excitation conditions. In the case of the QDs/Zn(bix) spheres, visualization of the localization of the QDs in the interior of the metal–organic particles by fluorescence microscopy is possible (see Figures S7 and S10 in the Supporting Information). This result has been further confirmed by TEM studies.

Encapsulation of multiple substances into solid matrices has also recently emerged as a promising strategy to confer multifunctional capabilities to systems for biomedical applications or simply for the development of novel materials.[25]

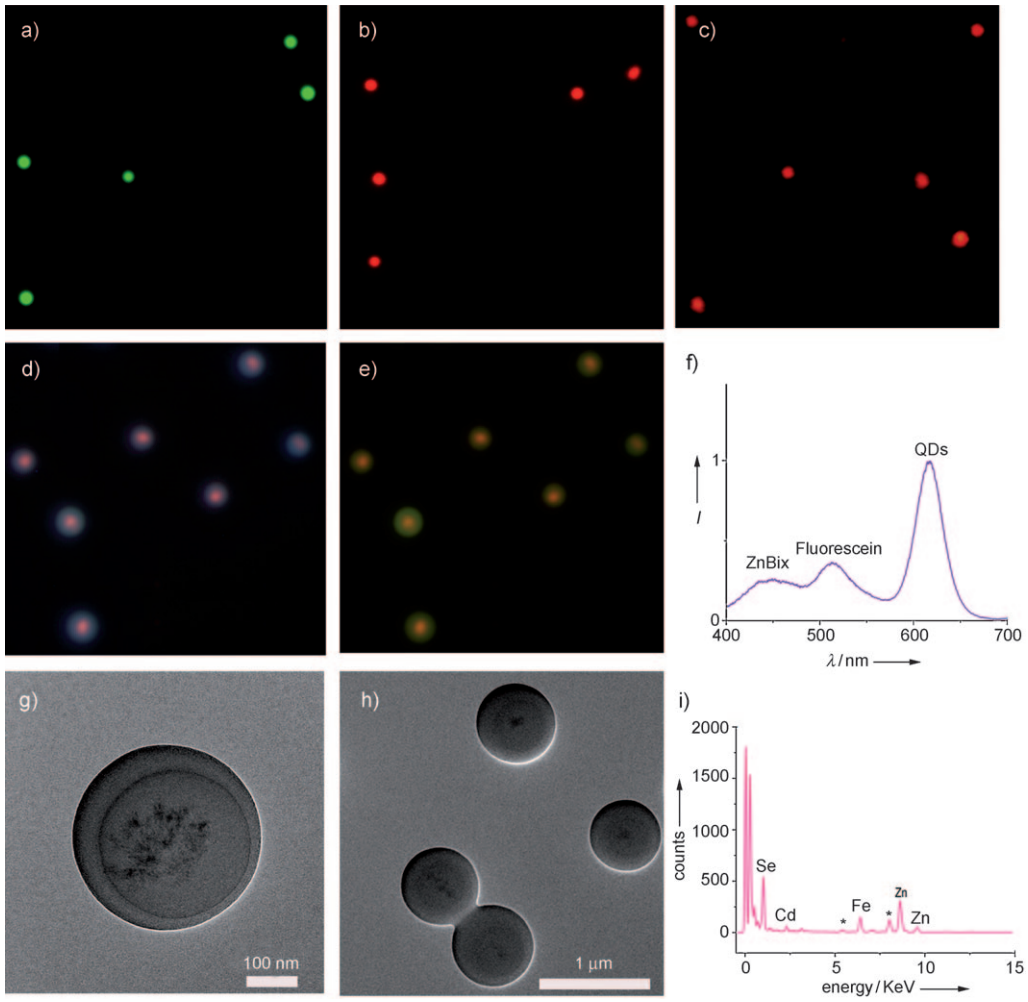

Figure 4. a–c) Fluorescence optical microscope images of fluorescein (λ_{exc} = 450–490 nm, λ_{em} > 515 nm), rhodamine B (λ_{exc} = 540–552 nm, λ_{em} > 590 nm), and QDs (λ_{exc} = 540–552 nm, λ_{em} > 590 nm) encapsulated within Zn(bix) spheres. d,e) Fluorescence optical microscope images of QDs/fluorescein/Zn(bix) spheres collected at different conditions: λ_{exc} = 359–371 nm and λ_{em} > 397 nm (d) and λ_{exc} = 450–490 nm and λ_{em} > 515 nm (e). Color-selective detection of the emitted fluorescence on a camera allows the Zn(bix) sphere (blue), fluorescein (green) and QDs (red) emission to be distinguished; the latter arises from the central part of the nanoparticles where the QDs are confined, as previously observed for QDs/Zn(bix) samples. f) Fluorescence emission spectra of QDs/fluorescein/Zn(bix) spheres measured at λ_{exc} = 355 nm, where both the metal–organic matrix and the encapsulated fluorophores absorb. g,h) High-resolution TEM images of QDs/iron oxide nanoparticles/Zn(bix) spheres. i) RX-EDX spectrum of QDs/iron oxide nanoparticles/Zn(bix) spheres, which shows the presence of zinc, iron, cadmium, selenium, and sulfur. The peaks marked with an asterisk arise from the TEM grid.

To provide evidence that metal–organic spheres can also be used for the encapsulation of more than one species, we first used Zn(bix) spheres for simultaneously embedding two luminescent compounds, such as QDs and fluorescein. Zn(bix) spheres that encapsulate both species were prepared by the addition of an aqueous solution of $Zn(NO_3)_2{\cdot}6H_2O$ to an ethanolic solution of bix containing QDs and fluorescein with stirring at room temperature. Interestingly, the resulting metal–organic spheres combine the intrinsic fluorescence properties of the metal–organic matrix with those characteristics of the encapsulated species. Therefore, QDs/fluorescein/Zn(bix) spheres are fluorescent in the blue, green, and red regions of the spectrum (Figure 4d–f). This allows the multiencapsulation of luminescent species into metal–organic particles to be envisaged as a potential route towards the development of tunable broadband light sources with applications in relevant fields such as display and laser fabrication.[26]

Following a similar synthetic methodology, Zn(bix) spheres that encapsulate luminescent QDs and magnetic iron oxide nanoparticles were also fabricated (Figure 4g,h). The encapsulation of both QDs and iron oxide nanoparticles was confirmed by RX-EDS microanalysis of individual Zn(bix) spheres, which showed that most of analyzed spheres contained zinc, iron, cadmium, selenium, sulfur, oxygen, nitrogen, and carbon (Figure 4i).

In summary, these results show that metal–organic micro- and nanospheres constitute a novel and very promising type of materials that can be used as functional matrices for the encapsulation of a large variety of substances. Functional metal–organic particles can be prepared with a wide diversity of metal ions and/or organic ligands.[16–21] Therefore, it is expected that this encapsulation approach will be extended to obtain metal–organic capsules that have novel functionalities. The combination of these capabilities with those of the encapsulated species open up new avenues in many fields, such as materials science and biotechnology, for the fabrication of novel and more complex multifunctional materials and carriers.

Experimental Section

All reagents were purchased from Aldrich Chemical Co., and used as received. The nonfunctionalized and water-soluble CdSe/ZnS QDs (Evitags) were purchased from Evident Technologies. 1,4-Bis(imidazol-1-ylmethyl)benzene (bix) was synthesized according to a previously reported procedure.[27] All HPLC quality solvents used were purchased from ROMIL, and used without further purification.

Encapsulation of functional species into Zn(bix) spheres was performed by the addition of a solution of $Zn(NO_3)_2{\cdot}6H_2O$ (150 mg, 0.5 mmol) in water (5 mL) to a solution of bix (121 mg, 0.5 mmol) in ethanol (25 mL), which also contained the desired species for encapsulation, with sonication or vigorous stirring at room temperature. The final concentrations of the encapsulated species in the reaction mixture were 4.5×10^{-4} M, 4×10^{-8} M, and 3.3×10^{-5} M for the magnetic iron oxide nanoparticles, QDs, and organic dyes, respectively. In all cases, the resulting encapsulated metal–organic systems were purified by centrifugation and washed three times with ethanol. The encapsulated systems were finally redispersed in ethanol to obtain the corresponding colloidal solutions.

Received: August 28, 2008
Published online: December 23, 2008

Keywords: coordination polymers · fluorescence · host–guest systems · magnetic properties · metal–organic particles

[1] R. Langer, *Nature* **1998**, *392*, 5–10.
[2] T. M. Allen, P. R. Cullis, *Science* **2004**, *303*, 1818–1821.
[3] J. R. Lindner, *Nat. Rev. Drug Discovery* **2004**, *3*, 527–532.
[4] D. F. Emerich, C. G. Thanos, *Expert Opin. Biol. Ther.* **2003**, *3*, 655–663.
[5] D. Nguyen, H. S. Zondanos, J. M. Farrugia, A. K. Serelis, C. H. Such, B. S. Hawkett, *Langmuir* **2008**, *24*, 2140–2150.
[6] M. Werts, M. Badila, C. Brochon, A. Hébraud, G. Hadziioannou, *Chem. Mater.* **2008**, *20*, 1292–1298.
[7] a) F. M. Muggia, J. D. Hainsworth, S. Jeffers, P. Miller, S. Groshen, M. Tan, L. Roman, B. Uziely, L. Muderspach, A. Garcia, A. Burnett, F. A. Greco, C. P. Morrow, L. J. Paradiso, L.-J. Liang, *J. Clin. Oncol.* **1997**, *15*, 987–993; b) D. D. Lasic, D. Papahadjopoulos, *Science* **1995**, *267*, 1275–1276.
[8] C. Lucas-Abellán, I. Fortea, J. M. López-Nicolás, E. Núñez-Delicado, *Food Chem.* **2007**, *104*, 39–44.
[9] K. A. Janes, M. P. Fresneau, A. Marazuela, A. Fabra, M. J. Alonso, *J. Controlled Release* **2001**, *73*, 255–267.
[10] a) J. Panyam, V. Labhasetwar, *Adv. Drug Delivery Rev.* **2003**, *55*, 329–347; b) B. J. Nehilla, P. G. Allen, T. A. Desai, *ACS Nano* **2008**, *2*, 538–544.
[11] a) J. M. J. Fréchet, *J. Polym. Sci. Part A* **2003**, *41*, 3713–3725; b) S. Svenson, D. A. Tomalia, *Adv. Drug Delivery Rev.* **2005**, *57*, 2106–2129.
[12] a) R. S. Ruoff, D. C. Lorents, B. Chan, R. Malhotra, S. Subramoney, *Science* **1993**, *259*, 346–348; b) X. Li, J. St. John, J. L. Coffer, Y. Chen, R. F. Pinizzotto, J. Newey, C. Reeves, L. T. Canham, *Biomed. Microdevices* **2000**, *2*, 265–272; c) J. Yang, J. Lee, J. Kang, K. Lee, J.-S. Suh, H.-G. Yoon, Y.-M. Huh, S. Haam, *Langmuir* **2008**, *24*, 3417–3421.
[13] a) S. Kitagawa, R. Kitaura, S.-i. Noro, *Angew. Chem.* **2004**, *116*, 2388–2430; *Angew. Chem. Int. Ed.* **2004**, *43*, 2334–2375; b) C. Janiak, *Dalton Trans.* **2003**, 2781–2804; c) N. R. Champness, *Dalton Trans.* **2006**, 877–880; d) P. Horcajada, C. Serre, M. Vallet-Regí, M. Sebban, F. Taulelle, G. Férey, *Angew. Chem.* **2006**, *118*, 6120–6124; *Angew. Chem. Int. Ed.* **2006**, *45*, 5974–5978; e) M. Eddaoudi, D. B. Moler, H. Li, B. Chen, T. M. Reineke, M. O'Keeffe, O. M. Yaghi, *Acc. Chem. Res.* **2001**, *34*, 319–330; f) D. Maspoch, D. Ruiz-Molina, J. Veciana, *Chem. Soc. Rev.* **2007**, *36*, 770–818.
[14] W. J. Rieter, K. M. L. Taylor, H. An, W. Lin, W. Lin, *J. Am. Chem. Soc.* **2006**, *128*, 9024–9025.
[15] a) S. Vaucher, M. Li, S. Mann, *Angew. Chem.* **2000**, *112*, 1863–1866; *Angew. Chem. Int. Ed.* **2000**, *39*, 1793–1796; b) E. Coronado, J. R. Galaín-Mascaroís, M. Monrabal-Capilla, J. García-Martínez, P. Pardo-Ibaíñez, *Adv. Mater.* **2007**, *19*, 1359–1361.
[16] M. Oh, C. A. Mirkin, *Nature* **2005**, *438*, 651–654.
[17] X. Sun, S. Dong, E. Wang, *J. Am. Chem. Soc.* **2005**, *127*, 13102–13103.
[18] a) H. Maeda, M. Hasegawa, T. Hashimoto, T. Kakimoto, S. Nishio, T. Nakanishi, *J. Am. Chem. Soc.* **2006**, *128*, 10024–10028; b) K. H. Park, K. Jang, S. U. Son, D. A. Sweigart, *J. Am. Chem. Soc.* **2006**, *128*, 8740–8741; c) H. Wei, B. Li, Y. Du, S. Dong, E. Wang, *Chem. Mater.* **2007**, *19*, 2987–2993; d) S. Jung, M. Oh,

Angew. Chem. **2008**, *120*, 2079 – 2081; *Angew. Chem. Int. Ed.* **2008**, *47*, 2049 – 2051.
[19] M. Oh, C. A. Mirkin, *Angew. Chem.* **2006**, *118*, 5618 – 5620; *Angew. Chem. Int. Ed.* **2006**, *45*, 5492 – 5494.
[20] Y.-M. Jeon, G. S. Armatas, J. Heo, M. G. Kanatzidis, C. A. Mirkin, *Adv. Mater.* **2008**, *20*, 2105 – 2110.
[21] I. Imaz, D. Maspoch, C. Rodríguez-Blanco, J.-M. Pérez-Falcón, J. Campo, D. Ruiz-Molina, *Angew. Chem.* **2008**, *120*, 1883 – 1886; *Angew. Chem. Int. Ed.* **2008**, *47*, 1857 – 1860.
[22] Q. Zhao, H. Li, X. Wang, Z. Chen, *Chem. Lett.* **2002**, 988 – 989.
[23] a) Z. Tian, J. Lin, Y. Su, L. Wen, Y. Liu, H. Zhu, Q.-J. Meng, *Cryst. Growth Des.* **2007**, *7*, 1863 – 1867; b) L. Wen, Y. Li, Z. Lu, J. Lin, C. Duan, Q. Meng, *Cryst. Growth Des.* **2006**, *6*, 530 – 537.
[24] L. Ramírez, P. K. Landfester, *Macromol. Chem. Phys.* **2003**, *204*, 22 – 31.
[25] B. J. Nehilla, P. G. Allen, T. A. Desai, *ACS Nano* **2008**, *2*, 538 – 544.
[26] S. Zhou, N. Jiang, B. Zhu, H. Yang, S. Ye, G. Lakshminarayana, J. Hao, J. Qiu, *Adv. Funct. Mater.* **2008**, *18*, 1407 – 1413.
[27] P. K. Dhal, F. H. Arnold, *Macromolecules* **1992**, *25*, 7051 – 7059.

